Available online at www.sciencedirect.com
ScienceDirect
International Journal of Heat and Mass Transfer 51 (2008) 4204–4215
International Journal of HEAT and MASS TRANSFER
www.elsevier.com/locate/ijhmt

Numerical simulation of transient heat and mass transfer in a cylindrical evaporator of a loop heat pipe

M.A. Chernysheva *, Yu.F. Maydanik

Institute of Thermal Physics, Ural Branch of the Russian Academy of Sciences, Amundsen Street, 106, Yekaterinburg 620016, Russia

Received 18 September 2007; received in revised form 11 November 2007
Available online 21 March 2008

Abstract

The paper investigates the transient processes of heat and mass transfer in a cylindrical evaporator of a loop heat pipe (LHP) during the device start-up. One of the most "arduous" prestart situations, which is characterized by the absence of a liquid in the evaporator central core and filled vapor removal channels, has been considered. With such liquid distribution a successful start-up of an LHP becomes possible only after formation of the vapor phase in the vapor removal channels and their liberation from the liquid. The aim of the investigations is to determine conditions that ensure the boiling-up of a working fluid in vapor removal channels. The problem was solved by a numerical method. Simulation of start-up regimes has been performed for different heat loads and different structural materials of the evaporator. Copper, titanium and nickel wick have been examined. Calculations have been made for three different working fluids; water, ammonia and acetone. Account has been taken of the conditions of heat exchange between the compensation chamber and surrounding medium.

Keywords: Loop heat pipe; LHP start-up; Heat and mass transfer; Temperature field; Evaporation; Boiling-up

1. Introduction

A loop heat pipe is a highly efficient heat-transfer device (see Fig. 1) which does not require any additional regulating actions from the outside for ensuring its serviceability [1]. It is a completely self-contained system capable of transferring heat for considerable distances and at different orientations in the gravity field. The heat load value therewith may vary in a sufficiently wide range. LHPs have found application in many fields of technology, where they are used as the key unit in the cooling systems of heat-tensioned elements.

One of the LHP advantages is its ability to start-up without resort to any additional auxiliary means. Upon completion of a start-up the device passes into the main, stationary operating mode, which is characterized by a stable circulation of a working fluid in the device, owing to which the heat transfer from the evaporation into the condensation zone is realized. However, for the beginning of circulation it is necessary that the heat load value should exceed a certain minimum level. The authors of Refs. [2–9] point out that the value of the minimum heat load required for a start-up, as well as the LHP behavior during it, depend on the device design features, the thermophysical characteristics of the materials used, environmental conditions, and also the initial distribution of a working fluid in the device. These conclusions were made on the basis of analysis of experimental results.

At the same time few publications are devoted to theoretical description and analytical investigation of starting regimes [10–12]. Appearingly it is connected with the fact that despite the apparent simplicity of the design and the well-known physical principles underlying the device functioning, the processes that proceed in characteristic segments of an LHP are interdependent and, therefore, rather complicated for analytical investigation. Thus, during an LHP start-up there exists interrelation between

* Corresponding author. Tel.: +7 343 2678 791; fax: +7 343 2678 799.
E-mail address: maidanik@etel.ru (M.A. Chernysheva).

0017-9310/$ - see front matter © 2008 Elsevier Ltd. All rights reserved.
doi:10.1016/j.ijheatmasstransfer.2007.12.021

Nomenclature

A	accommodation coefficient
c	specific heat capacity, J/kg K
G	mass flow rate, kg/s
h	evaporation heat, J/kg
k	thermal conductivity, W/m K
Q	heat load, W
q	density of heat load, W/m^2
j	mass evaporation rate, kg/m^2 s
L	length, m
M^*	molecular weight, kg/mol
P	pressure, Pa
R^*	universal gas constant, 8.31 J/mol K
R	substance gas constant, J/kg K
r	radial coordinate
T	temperature, °C

Greek symbols

α	heat-transfer coefficient, W/m^2 K
τ	time, s
ν	kinematic-viscosity coefficient, m^2/s
μ	dynamic-viscosity coefficient, Pa s
ρ	density, kg/m^3
ε	porosity

Subscripts and superscripts

amb	outside ambient
c	chamber filled with vapor
core	central core
cc	compensation chamber
cond	condenser
ev	evaporation
ext	external
ef	effective
l	liquid
nq	barrier layer of wick
nucl	nucleation
oh	overheating or overshoot
ps	porous structure
v	vapor
vl	vapor line
wick	wick
wall	evaporator body

hydrodynamic and thermal processes. Besides, simulation of an LHP start-up which would be fully identical to the actual pattern proves to be very difficult since even with the observance of extreme accuracy of analytical description of heat-and-mass-transfer processes some uncertainty is always present. This uncertainty is connected with the prestart distribution of a working fluid, which in actual conditions depends on the LHP history, the device orientation and the environmental thermal conditions. As distinct from a CPL, in an LHP no special prestart procedures are performed for forced redistribution of a liquid inside the device with the aim of a guaranteed filling of the evaporator before a start-up. Therefore it is possible to predict where the liquid will be at the instant of the start-up only to a certain degree of probability. In such a case the only rational approach to the solution of this problem is revealing and systematizing typical prestart situations, whose investigation will make it possible to obtain some additional information, on the basis of which conclusions will be formulated and useful recommendations will be elaborated.

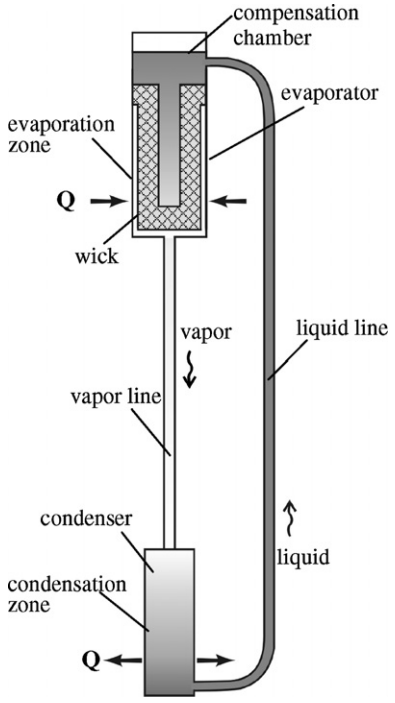

Fig. 1. Scheme of a loop heat pipe.

In Ref. [2] one can find a classification of the four main types of prestart situations in the LHP evaporator and description of the start-up scenario for each of them. The authors note that the device start-up is sufficiently easy when the evaporation zone, which is situated close to the LHP evaporator wall, has been formed by the instant of the start-up, with the vapor removal channels free of liquid. In this case the LHP start-up proceeds as follows. After a heat load supply the evaporator begins to warm up. An immediate response to increasing temperature is the liquid evaporation from the wick menisci into the vapor removal channels, through which the forming vapor is evacuated from the evaporator into the vapor line. The process of generation of vapor and its further expansion lead to liberation of the whole vapor line and some part of the condenser from the liquid, which is pushed out into the

compensation chamber (CC). Owing to the redistribution of the working fluid, in the condenser there forms a free surface required for complete vapor condensation. The area of this surface depends on the conditions of the condenser cooling, and also on the amount of heat supplied to the evaporator and then spent for the evaporation. The condensate formed enters the CC through the liquid line, soaks into the wick and filters through it to the evaporation zone. To maintain the circulation, it is necessary to ensure a certain pressure drop ΔP_{ext} between the evaporation zone and the compensation chamber, which also forms in the start-up process:

$$\Delta P_{ext} = \Delta P_v + \Delta P_l, \tag{1}$$

where ΔP_v and ΔP_l are pressure losses during the vapor and the liquid motion from the evaporation surface to the compensation chamber.

The start-up process takes some time. Experimental investigations show that the higher the heat load supplied, the shorter time is required for the device to go into a stationary operating regime. The temperature diagram in Fig. 2a shows the characteristic behavior of the LHP operating temperature during a start-up from a state with a completed evaporation zone. It is seen that a start-up in this case proceeds smoothly enough. At first the temperature increases intensively, then its increase slows down, and some time later its value is fixed at a certain constant level.

Quite a different character of the operating temperature behavior is observed when an LHP is started from a state with flooded vapor removal channels (see Fig. 2b) and when there is no vapor–liquid interface in the evaporation zone. In this case there is a peak on the temperature curve. Since the peak value of the operating temperature may exceed considerably the temperature value of an LHP operating in a stationary regime, such a start-up scenario is often called "a start-up with temperature overshoot".

The main reason for a start-up with overshoot is the fact that the evaporation zone is not formed yet by the beginning of the LHP operation. This complicates considerably the start-up process, which in such a case may be arbitrarily divided into two stages. At the first stage conditions for liquid boiling-up in the vapor removal channels are created. Then follows the second stage, which begins with the instant of formation of the vapor phase in the evaporation zone. At the expense of the abrupt vapor expansion the liquid is driven out of the vapor removal channels, the vapor line and part of the condenser into the compensation chamber. At the same time the required balance of pressures and temperatures in the evaporation zone and in the compensation chamber (1) is created. It ensures the working fluid circulation in the LHP. After a successful start-up there comes a stationary regime of the LHP operation, which is characterized by the constancy of operating temperatures.

Both of the start-up stages are distinctly seen on the temperature curve. The first stage is characterized by a continuous temperature rise and ends at the instant the temperature reaches its maximum value. The second stage begins with an abrupt temperature drop and ends in its stabilization, which means that the start-up has been successful, and the stable circulation of the working fluid does exist. If at the first stage it is impossible to create appropriate conditions for the boiling-up of a working fluid in the vapor removal channels, it becomes impossible to realize an LHP start-up. In this case a continuous increase in the operating temperature is observed. The closing stage of the start-up is absent, so no transition into a stationary operating regime takes place.

According to the nucleation evaporation theory [13], for the origination of viable vapor bubbles of radius r_{cr} and their further growth it is necessary that the liquid in the vapor removal channels should be superheated with respect to its equilibrium state by the value of ΔT_{nucl} which can be evaluated by the following formula:

$$\Delta T_{nucl} = \frac{2 \cdot \sigma \cdot T}{r_{cr} \cdot h \cdot \rho_v}. \tag{2}$$

In our case it means that it is necessary to create a certain temperature difference between the liquid temperature at the external wick surface T_2 (Fig. 3) and the vapor temperature T_∞ outside this zone

$$\Delta T = T_2 - T_\infty, \tag{3}$$

which would exceed the value of ΔT_{nucl}, i.e.

$$\Delta T \geqslant \Delta T_{nucl}. \tag{4}$$

The required temperature drop ΔT is formed at the first stage of the start-up, when after the switching of a heat

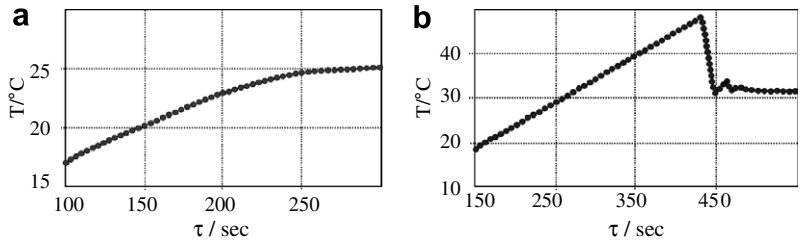

Fig. 2. Behavior of the operating temperature during a start-up: (a) start-up without overshoot; (b) start-up with overshoot.

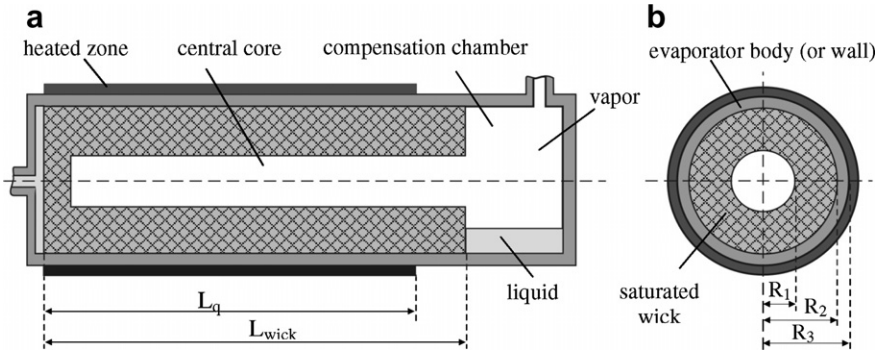

Fig. 3. Scheme of LHP's evaporator (a, b) and domain for computational model (b).

load the evaporator gradually begins to warm up, and the temperature T_2 increases.

Experiments have shown that the success of the procedure of initiation of the liquid boiling-up depends on the heat flux supplied to the evaporator, the relation between the main design dimensions of the evaporator, on the thermophysical properties of the materials used and the working fluid, and also on the intensity of heat exchange with the environment. At low densities of the heat flow q the period of "expectation" of boiling-up may take an appreciable length of time. Owing to the prolonged first stage the whole start-up process is eventually protracted. At low densities of the heat flow q the start-up may last for quite a long time, about 30 min and more. Another hazard connected with a protracted start-up is the fact that with a prolonged evaporator heating and a considerable rise of temperature the thermal state of the object being cooled may exceed a certain maximum allowable level.

There is a range of relatively low heat loads at which the minimum superheat ΔT, required for a start-up, cannot be achieved at all, i.e. the condition (4) cannot be fulfilled. In this case one can also observe a continuous rise of the operating temperature, whose value may become critical. For this reason quite important is the evaluation of the minimum start-up heat load at different LHP operating conditions.

There are two prestart situations in which the vapor removal channels are filled with a liquid. The distinctive feature of one of them is the fact that the liquid fills the whole evaporator. Such a prestart situation is possible at LHP orientations with slopes $\phi < 0°$, when the evaporator is below the condenser. Besides, a complete filling of the evaporator may be caused by peculiar temperature conditions, viz. if the temperature of the condenser before a start-up proves to be higher then the evaporator temperature. The peculiarities of the LHP start-up with a filled evaporator are considered in Ref. [11], where the problem of formation of a temperature field in a cylindrical evaporator is solved by a numerical method.

The present paper studies a different prestart case with filled vapor removal channels, which is characterized by the absence of a liquid in the evaporator central core. Such a liquid distribution may arise when the amount of the working fluid filled has been chosen incorrectly. If the bulk of the working fluid in the LHP is smaller than the optimum one, at some device orientations there may be no liquid in the central core, but at the expense of the capillary forces it is retained in the vapor removal channels. The aim of the present investigations is to simulate the thermal processes in the evaporator during the first stage of the start-up and to determine conditions that ensure the boiling-up of a working fluid in vapor removal channels.

Since expression (3), which determines ΔT, is formulated in the general form, in concretizing it for the prestart situation examined here one should write ΔT as the difference between the temperature at the external surface of the wick T_2 and the vapor temperature in the central core and compensation chamber T_c:

$$\Delta T = T_2 - T_c. \tag{5}$$

It should also be mentioned that such a prestart liquid distribution in an evaporator with an interface situated at the internal surface of the wick is quite dangerous as it may be the reason for the LHP operation with the so-called reverse circulation of a working fluid. In this case the inner surface of the wick is the evaporation zone, and the replenishment with a liquid is realized through the wick outer surface. A similar scheme of co-directed flows of heat and liquid moving towards the centre is used in the evaporation zone of conventional heat pipe.

2. Setting up the problem and the main assumptions of the model

The scheme of a cylindrical evaporator with indication of the zone of heat load supply is given in Fig. 3. The heating zone is shifted in the direction opposite to the compensation chamber and is separated from it by a barrier layer, which serves as an obstacle to penetration of heat and vapor from the heating zone into the CC. The length of the barrier layer L_{nq} is determined as the difference between the wick length L_{wick} and the length of the heating zone L_q: $L_{nq} = L_{wick} - L_q$. We will consider the uniform distribution of the heat load, then the heat load density q will be determined as:

$$q = \frac{Q}{2 \cdot \pi \cdot R_3 \cdot L_q}, \tag{6}$$

where Q is the heat load, R_3 is the evaporator radius.

Let us consider the problem of the evaporator heating up provided that at the instant of time $\tau = 0$ the liquid fills the vapor removal channels and saturates the wick. In the central core there is no liquid. In the compensation chamber the liquid is absent altogether or there is a small amount of it, for instance, as is shown in Fig. 3. Owing to the fact that the level of the liquid accumulated in the lower part of the compensation chamber is below the central core the liquid cannot get into it. The boundary between the vapor and the liquid the porous structure is saturated with is situated at the inner surface of the wick ($r = R_1$).

At the initial instant of time $\tau = 0$ the temperature field of the evaporator is uniform $T(r,0) = T_0$. The liquid and the vapor in proximity to a surface with the radial coordinate $r = R_1$ are in the state of thermodynamic equilibrium, there is no evaporation, and therefore $q_{ev} = 0$. After the supply of heat load Q the evaporator temperature begins to rise. The thermal front moves from the outer surface of the evaporator ($r = R_3$) to its centre and some time later reaches the inner surface of the wick ($r = R_1$). The liquid begins to evaporate from the surface of the menisci facing the central core. The mass evaporation rate is calculated by the following formula [14]:

$$j_{ev} = A \cdot (P_1 - P_c) \cdot \left(\frac{M^*}{2 \cdot \pi \cdot R^* \cdot T_1}\right)^{1/2}, \tag{7}$$

where A is the accommodation coefficient, P_c is the vapor pressure away from the vapor–liquid interface, P_1 is the pressure near the vapor–liquid interface, which is determined from the equation of phase equilibrium $P_1 = f(T_1^s)$.

With allowance made for the uniform heat supply and the sufficiently extended length of the active zone, we will consider a one-dimensional problem, which takes into account only the radial component of the heat flow, i.e. the edge effects connected with the manifestation of nonlinearity in the butt-end sections of the wick in such a case have only a slight influence on the overall picture of preferential heat distribution only in the radial direction.

We believe that the intrapore heat-transfer coefficient is high enough, therefore the temperature of the wick and the liquid in the pores in every sufficiently small elementary volume is the same. Heat transfer from the heating zone ($r = R_3$) to the evaporation surface ($r = R_1$) is initially realized at the expense of the thermal conductivity of the evaporator wall k_{wall}, and then at the expense of the effective thermal conductivity of a wetted wick:

$$k_{wick} = k_l \cdot \varepsilon + k_{ps} \cdot (1 - \varepsilon). \tag{8}$$

The amount of the working fluid evaporated from the inner surface of the wick ($r = R_1$) is compensated for by the same amount of the liquid which arrives at the wick from the vapor removal channels, therefore the wick is not deprimed. The liquid infiltration to the evaporation surface is realized at the expense of capillary forces. The flow rate of working fluid in the wick is low, so the convective component of heat transfer is not taken into account. The temperature field that forms in the process of the evaporator heating $T = f(r,\tau)$ will determine the temperature drop required for the boiling-up of the working fluid in the vapor removal channels.

3. Mathematical formulation of the problem

The mathematical model of heat-and-mass transfer processes in the evaporator with allowance for the assumptions adopted is described by the following equations: the energy equation for the evaporator wall (zone $R_2 < r < R_3$):

$$\rho_{wall} \cdot c_{wall} \cdot \frac{\partial T}{\partial \tau} = k_{wall} \cdot \left(\frac{\partial^2 T}{\partial r^2} + \frac{1}{r}\frac{\partial T}{\partial r}\right), \tag{9}$$

and the energy equation for a saturated wick (zone $R_1 < r < R_2$):

$$\rho_{wick} \cdot c_{wick} \cdot \frac{\partial T}{\partial \tau} = k_{wick} \cdot \left(\frac{\partial^2 T}{\partial r^2} + \frac{1}{r}\frac{\partial T}{\partial r}\right). \tag{10}$$

The effective thermal conductivity of a saturated wick is determined according to expression (8). The product of the first two cofactors on the left-hand side of Eq. (10) may be presented as follows:

$$\rho_{wick} \cdot c_{wick} = \rho_l \cdot c_l \cdot \varepsilon + \rho_{ps} \cdot c_{ps} \cdot (1 - \varepsilon). \tag{11}$$

Presented below are the initial and the boundary conditions.

At the initial instant of time $\tau = 0$:

$$T(r,0) = T_0, \quad P_c = P^s(T_0). \tag{12}$$

At the external boundary $r = R_3$ we set the density of heat flow calculated by (6):

$$k_{wall} \cdot \frac{\partial T}{\partial r} = -q. \tag{13}$$

At the boundary between the capillary structure and the evaporator wall ($r = R_2$) on the assumption that the wick has an ideal thermal contact with the evaporator wall the boundary condition will look like:

$$k_{wall}\frac{\partial T}{\partial r} = k_{wick}\frac{\partial T}{\partial r}. \tag{14}$$

The equation of thermal interaction of phases at a vapor–liquid interface ($r = R_1$) is written as a follows:

$$-k_{wick} \cdot \left.\frac{\partial T}{\partial r}\right|_{R_1} = j_{ev} \cdot h, \tag{15}$$

where h is the specific evaporation heat. The vapor pressure away from the evaporation surface P_c is present in expression (7) for a flow of evaporating liquid j_{ev}. The role of this parameter is very important as the intensity of evaporation and, consequently, the amount of heat absorbed in a

liquid–vapor phase transition depend on its value. The greater amount of liquid evaporates, the more intensive is the "cooling" of the inner surface of the wick. The heat-transfer conditions at the boundary $r = R_1$ affect the formation of the temperature field in the wick and, correspondingly, the value of the temperature drop ΔT. The vapor pressure P_c may be determined from the equation of state:

$$P_c = \rho_v \cdot R \cdot T_c, \tag{16}$$

where ρ_v is the density of vapor away from the evaporation surface. In the process of the evaporator heating ρ_v may change owing to changes in the vapor mass m:

$$\frac{d\rho_v}{d\tau} = \frac{1}{V_v}\frac{dm}{d\tau}, \tag{17}$$

where V_v is the volume occupied by vapor. Designating the initial vapor mass as m_0, we write an expression for the vapor mass at any subsequent instant of time $\tau = \tau_0 + \Delta\tau$ in the form:

$$m = m_0 + \Delta m_{ev} - \Delta m_{cond}, \tag{18}$$

where Δm_{ev} is the increment in the vapor mass at the expense of the liquid evaporated from the inner surface of the wick, Δm_{cond} is the mass of the vapor condensed. If the CC is thermally insulated, and there is no condensation at its cold inner surface, we have:

$$m = m_0 + \Delta m_{ev}. \tag{19}$$

The amount of the working fluid evaporated is described by the following expression:

$$\Delta m_{ev} = \int S_1 \cdot j_{ev}(\tau) \cdot d\tau, \tag{20}$$

where S_1 is the area of the wick inner surface. In the conditions of heat exchange between the CC and the environment the CC surface is cooled, which causes vapor condensation at the inner surface of the CC:

$$\Delta m_{cond} = \frac{1}{h} \cdot \int Q_{amb}(\tau) d\tau, \tag{21}$$

where Q_{amb} is the heat flow dissipated from the outer surface of the compensation chamber S_{cc_ext} into the environment, whose temperature is T_{amb}:

$$Q_{amb} = \alpha_{amb} \cdot S_{cc\_ext} \cdot (T_c - T_{amb}). \tag{22}$$

The area of the surface S_{cc_ext} depends on the geometric dimensions of the compensation chamber:

$$S_{cc\_ext} = \pi \cdot R_3^2 + 2 \cdot \pi \cdot R_3 \cdot L_{cc}, \tag{23}$$

where L_{cc} is the CC length determined by the formula:

$$L_{cc} = \frac{V_{cc}}{\pi \cdot R_2^2} + \delta_{cc}. \tag{24}$$

The second component in (24) takes into account the thickness of the butt-end cover of the compensation chamber. The vapor temperature in the chamber filled with vapor is determined from the heat balance:

$$Q_{amb} + Q_{eb} + Q_{ev} = 0, \tag{25}$$

where Q_{eb} is the heat flow in the compensation chamber through the evaporator body:

$$Q_{eb} = \frac{k_{wall}}{L_{nq} + 0.5 \cdot L_{cc}} (T_3 - T_c) \cdot \pi \cdot (R_3^2 - R_2^2). \tag{26}$$

The third term in (25) takes into account the increment in the heat at the expense of the evaporated mass of vapor with temperature T_1, which is higher than the temperature of vapor T_c in the CC. Usually a value Q_{ev} is very small as against Q_{amb} and Q_{eb} consequently it may be ignored.

Since the vapor is in both the central core and the compensation chamber, the total volume V_c occupied by vapor is determined by the formula

$$V_c = V_{core} + V_{cc} \cdot (1 - \zeta), \tag{27}$$

where V_{core} is the volume of the central core, V_{cc} is the volume of the compensation chamber, ξ is the parameter which takes into account the degree of filling the CC with liquid. If only vapor is present in the CC, i.e. if there is no "puddle" of liquid there, then $\xi = 0$.

The dimensions of the central core and consequently, its volume V_{core} are determined by the geometric dimensions of the evaporator itself, whereas the volume of the CC depends on the dimensions of the vapor line and the condenser, i.e. it is determined by the dimensions of the LHP constructional elements, which are external with respect to the evaporator. The CC dimensions are determined from the condition of correspondence of volumes, according to which the CC volume may not be smaller than the sum of the volumes of the vapor line V_{vl} and the condenser V_{cond}:

$$V_{cc} \geqslant V_{vl} + V_{cond}. \tag{28}$$

The dimensions of the vapor line and the condenser may vary widely depending on the heat-transfer length and the condenser design, which was chosen by the criterion of maximum adaptation to the conditions of heat rejection at minimum mass-and-size characteristics of the condenser-heat exchanger.

Since the CC dimensions may be different, the present model problem should be classified as a multivariant one, and it leads to the necessity of solving this problem for different values of V_{cc} because only in this case there is a possibility to obtain a sufficient body of data for a qualitative comparative analysis of various possible situations that take place during the LHP start-up. Besides, the degree of multivariantability of the model problem may increase many times because of the necessity of taking into account the conditions of heat exchange of the compensation chamber with the environment, which, generally speaking, may be different.

For a comprehensive investigation of the start-up problem it is necessary that calculations should be made for different variants of model problems. Such an approach, however, is inefficient from the viewpoint of unreasonably

high expenses for a great number of numerical experiments. To obtain maximum informativeness from the results of calculations with their minimum number, we will do the following. Calculations will be made only for two variants of the model problem, which are maximally idealized and at the same time so opposite in description that they may be regarded as limiting, restricting the whole spectrum of possible problems. Then the results obtained will restrict the area of solution of all intermediate problems.

The first variant of the "boundary" problem may be characterized in the following way. We believe that the pressure P_c does not change with time. Such a state may be observed for evaporators with a large thermal resistance of the evaporator body and with a large CC the outer surface of which is not thermally insulated ($\alpha_{amb} \neq 0$). In intense processes of heat transfer into the environment the temperature and consequently the pressure inside the chamber remain constant $P_c = \text{const}$. Vapor condensation is observed at the inner "cold" surface of the CC:

$$j_{ev} = j_{cond}. \tag{29}$$

In describing the second "boundary" problem we assume that the pressure in the chamber differs little from that at the boundary with the coordinates $r = R_1$. Such a state may take place if the CC volume is very small, and the outer surface is thermally insulated, i.e. $V_{cc} \approx 0$ and $\alpha_{amb} = 0$.

4. Procedure of numerical solution

A system of differential equations was solved numerically. The energy balance method was chosen for obtaining a numerical formulation of the problem of heat propagation in a cylindrical evaporator in the radial direction. In numerical realization of the solution use was made of a uniform grid for the time coordinate and a piecewise uniform grid for the spatial coordinate r for two subregions of the computational domain. The first subregion is the space of the evaporator wall, the second is the wick zone. The length of the space step for each of the subregions was chosen with allowance for two requirements: saving of the counting time and sufficiency of the number of nodes in every computational subregion. The calculation of the temperature field of the evaporator body and the wick was made at 8 and 20 nodal points, respectively.

5. Results of calculation, comparative analysis and discussion

The above model representations were used as a basis for calculations simulating the first stage of the LHP start-up in the absence of liquid in the wick central core and with flooded vapor removal channels. Calculations were made for the following initial data. The initial evaporator temperature T_0 and the ambient temperature T_{amb} were equal to 20 °C. The evaporator radius R_3, the wick radius R_2 and the radius of the central core R_1 equaled 12 mm, 10 mm and 2 mm, respectively. The evaporator active zone length L_q was 80 mm. The wick porosity ε was equal to 0.6. The starting heat load varied from 1 to 100 W. In this case the heat flux in the active zone varied from 166 W/m^2 to 16 600 W/m^2. The following combinations of materials were considered as structural materials for the evaporator as a composite object: copper body–copper wick (Cu–Cu); stainless steel body–nickel wick (SS–Ni), stainless steel body–titanium wick (SS–Ti). Calculations were made for three different working fluids; water, ammonia and acetone. Account was also taken of different conditions of heat exchange between the compensation chamber and the environment.

Fig. 4 shows how the thermophysical properties of structural materials may influence the temperature of the evaporator outer surface in the zone of heat load supply. Calculations were made for a model problem with the boundary conditions classified in Paragraph 3 as the first limiting case which envisages intense heat exchange between the CC and the environment. Presented as an example are the results of calculation for water as a working fluid and a heat load of 10 W, which corresponds to a heat flux equal to 1660 W/m^2. Calculations were also performed for other heat loads Q in the range from 1 to 100 W. In all cases the character of behavior of temperature curves $T_3 = f(\tau)$ was of the same type. The thermal conductivity of the copper, the nickel and the titanium wick k_{wick} was equal to 30, 7 and 3 W/m K, respectively. The thermal conductivity of the copper body equaled 380 W/m K and of the stainless steel body 17 W/m K. It can be seen from Graph 4 that at the same heat load supplied to the evaporator the temperature at its outer surface T_3 proves to be lower for evaporators made of more heat-conducting structural materials. More intense heat penetration into the interior of such evaporators finally ensures their more rapid and uniform warm up. This is confirmed by the results, which show how the temperature field varies with time for a copper evaporator and an evaporator which has a titanium wick and a stainless steel body (Fig. 6).

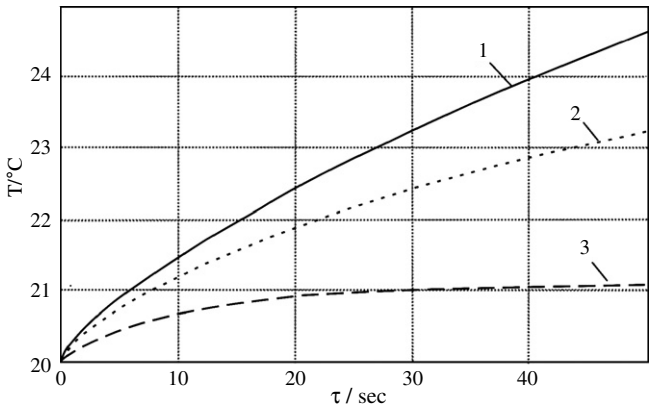

Fig. 4. Time dependence of the temperature at the evaporator external wall T_3 at a heat load of 10 W in conditions of intense heat exchange CC with the environment for evaporators of different materials: 1 – SS/Ti, 2 – SS/Ni, 3 – Cu/Cu. The working fluid is water.

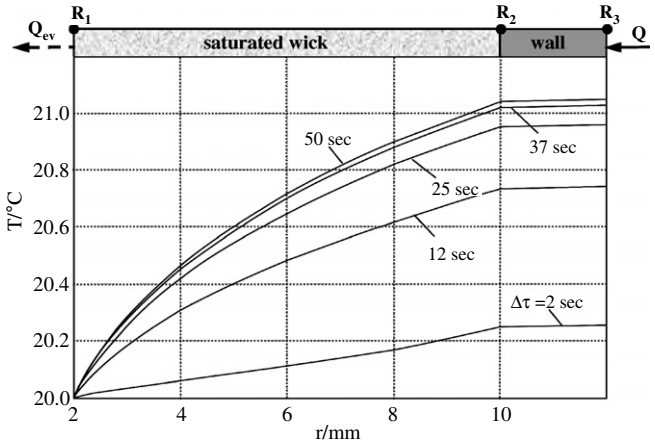

Fig. 5. Evolution of temperature field in Cu/Cu – evaporator in condition of intense heat exchange CC with the environment. The heat load is 10 W. The working fluid is water.

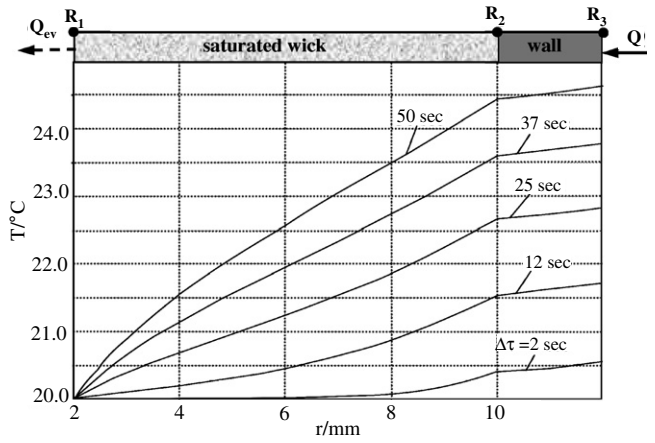

Fig. 6. Evolution of temperature field in SS/Ti – evaporator in condition of intense heat exchange CC with the environment. The heat load is 10 W. The working fluid is water.

Graphs $T = f(\tau)$ are presented for five time intervals elapsed after the instant of switching on the heat load Q. A comparison of Figs. 5 and 6 makes it possible as well to explain the difference in the behavior of the curves in Fig. 4, according to which the temperature at the outer surface of the copper evaporator 50 s after switching on the heat load is hardly changed, whereas the temperature of the two other evaporators continues to increase. From Fig. 5 it is seen that by this time the temperature field in the copper evaporator changes only slightly. There is a well-defined tendency to temperature stabilization, owing to which arises an illusion that the LHP start-up is realized without temperature overshoot (see Fig. 2). In actual fact there is no circulation of the working fluid, it will be demonstrated later, and the LHP does not operate properly, though the thermal stabilization of the object to be cooled is realized, and the temperature of the heat-receiving surface approaches a stationary value. Such an effect is achieved at the cost of the high thermal conductivity of the materials and the balance of heat flows in the copper evaporator, which in this case acts as a heat-conducting element between the heat source and the environment into which this heat is dissipated.

It should be emphasized that such a scenario of a sufficiently rapid completion of transient processes can be observed only under highly intense heat exchange between the CC and the environment and at low densities of the heat flow supplied to an evaporator made of materials with a high thermal conductivity. At low intensity of heat exchange with the environment, when $\alpha_{amb} \approx 0$, which takes place, for instance, when operating in conditions of vacuum, one can observe a continuous increase of temperatures, as is demonstrated, in particular, in Fig. 7. An identical result of continuous heating of the evaporator may be observed when the CC is adequately thermally insulated.

We shall note once again that the results are presented for two limiting, i.e. maximally idealized conditions of heat exchange at the CC outer surface. From this it follows that the behavior of temperature curves $T_3 = f(\tau)$ for all other possible actual conditions, as well as the estimative values of temperatures, can be predicted by way of comparison of the corresponding temperature curves in Figs. 4 and 7.

Calculations also show that the conditions of heat exchange between the CC and the environment have a considerable effect on the value of ΔT, which forms in the process of the evaporator heating. Figs. 8 and 9 present the results of calculations for a copper evaporator. Its geometric parameters are described above. Water was used as a working fluid. Calculations were made for different heat loads Q. The curves $\Delta T = f(\tau)$ presented in Fig. 8 have been obtained with allowance for the intense heat exchange between the CC and the environment. Results for an identical copper evaporator but with a thermally insulated CC are given in Fig. 9.

For evaluating the minimum start-up load Q_{min} determined from the condition (4) in the graphs there are curves $\Delta T_{nucl} = f(\tau)$. The calculation of ΔT_{nucl} was made by

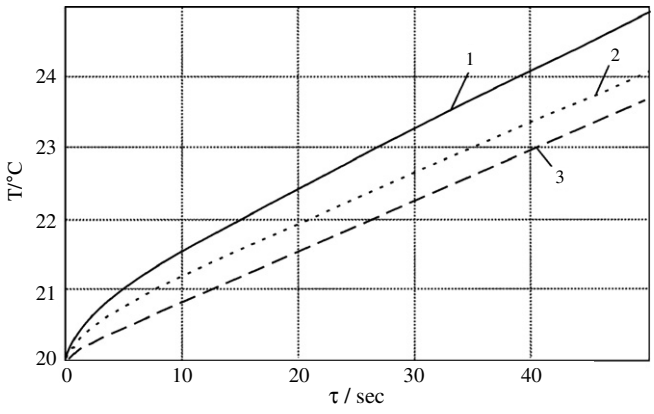

Fig. 7. Time dependence of the temperature at the external surface of the evaporator body T_3 at a heat load of 10 W for evaporators of different materials: 1 – SS/Ti, 2 – SS/Ni, 3 – Cu/Cu. Compensation chamber is heat-insulated. The working fluid is water.

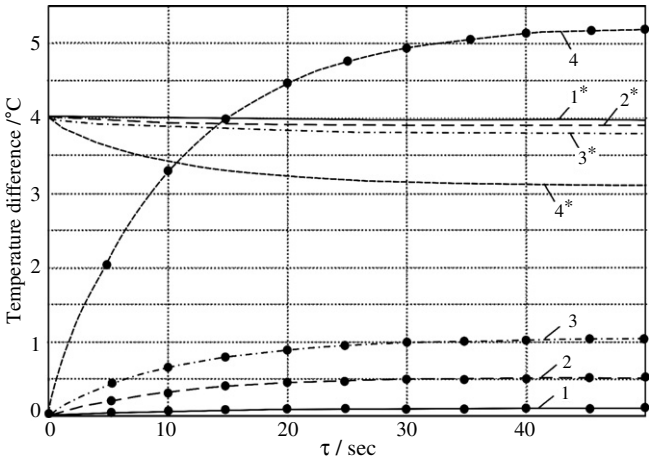

Fig. 8. Formation of temperature drop ΔT (curves 1–4) and variation of ΔT_{nucl} (curves 1^*, 2^*, 3^*, 4^*) in the process of heating of a copper evaporator (Cu/Cu) at different heat loads: 1, 1^* – $Q = 1$ W; 2, 2^* – $Q = 5$ W; 3, 3^* – $Q = 10$ W; 4, 4^* – $Q = 50$ W. The working fluid is water. The compensation chamber is not heat-insulated.

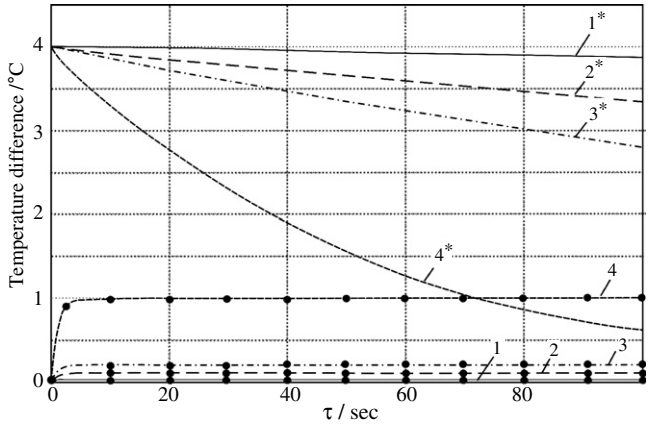

Fig. 9. Formation of temperature drop ΔT (curves 1, 2, 3) and variation of ΔT_{nucl} (curves 1^*, 2^*, 3^*) in the process of heating of a copper evaporator (Cu/Cu) at different heat loads: 1, 1^* – $Q = 1$ W; 2, 2^* – $Q = 5$ W; 3, 3^* – $Q = 10$ W; 4, 4^* – $Q = 50$ W. The working fluid is water. The compensation chamber is heat-insulated.

formula (2). The value equal to 0.25 mm, comparable with the characteristic size of the cross-section of the vapor removal channels, was taken for r_{cr}. Since the thermophysical characteristics of the working fluid depend on the temperature, and it varies in the process of the evaporator heating, this circumstance was taken into account in calculating ΔT_{nucl}, namely as $\Delta T_{\text{nucl}} = f(T_2(\tau, Q))$. Data on the variation of the working fluid temperature in the zone where the vapor removal channels were situated T_2 were taken from the results of a numerical experiment simulating the initial stage of an LHP start-up from the state with flooded vapor removal channels and in the absence of liquid in the central core. From the graphs presented it is seen that in start-up process the value of ΔT_{nucl} decreases, and it is a positive factor, which reflects the fact that with an increase in the liquid temperature the conditions for formation of a viable vapor bubble improve, and the probability of the liquid boiling-up in the vapor removal channels becomes higher. At the same time it should be mentioned that the decrease in ΔT_{nucl} is observed as long as the tendency for evaporator heating is retained, and accordingly there is an increase in the liquid temperature in the zone of location of vapor removal channels. Thus, from the graph in Fig. 8 it is seen that the state of thermal equilibrium for a copper evaporator with a CC that is not thermally insulated is achieved sufficiently fast, as has been mentioned above, it is promoted by the high intensity heat exchange between the CC and the environment. After the thermostabilization of the evaporator the value of ΔT_{nucl} does not change any longer. The same happens to the formation of the temperature difference ΔT. The value of ΔT increases as long as the thermal processes in the evaporator may be characterized as unsteady-state ones. After the stabilization of the temperature field of the evaporator the value ΔT in the course of time remains unchanged.

Analysis of the behavior of the curves $\Delta T = f(\tau)$ and $\Delta T_{\text{nucl}} = f(\tau)$ presented in Fig. 8 makes it possible to reveal the following regularities typical of the start-up of an LHP made of highly heat-conducting materials with an intense heat exchange with the environment. The higher the heat load Q supplied to the evaporator, the longer the time of transient thermal processes in the evaporator. Besides, with increasing heat load one can observe the tendency to mutual approaching of the curves ΔT and ΔT_{nucl}. Taking into account the behavior of the corresponding curves ΔT and ΔT_{nucl}, and also comparing their mutual arrangement, it is possible to predict how successfully the start-up will end. The criterion of a successful start-up is the condition (4). It is seen that for low heat loads, such as 1, 5 and 10 W, the condition (4) cannot be fulfilled. It means that favorable conditions for the liquid boiling-up in the vapor removal channels cannot be created, and therefore it becomes impossible to organize the circulation of a working fluid and realize an LHP start-up. At the same time it can be seen that a heat load $Q = 50$ W proves to be acceptable for a successful LHP start-up. It takes a little more than 10 s for the value of ΔT to increase to an extent that it becomes equal to the value of ΔT_{nucl}, and then exceeds it. After the curves designated in the graph as 4 and 4^* intersect, one should expect the liquid boiling-up, which will ensure the vacation of the vapor removal channels.

In the absence of heat exchange with the environment the time of boiling-up expectation increases. Thus, for instance, for a load of 50 W the period preceding the instant of boiling-up according to Fig. 9 exceeds 70 s, and this is seven times longer than during intense heat exchange between the compensation chamber and the environment. Another distinction from the previous example is the reduction of the time interval within which the value of ΔT varies. The maximum value of the temperature drop ΔT in this case proves to be much smaller than the maximum value of ΔT obtained at the same heat loads, but with

allowance for the heat exchange between the CC and the environment.

An analysis of the results presented in Fig. 8 has revealed the adverse effect that the intense heat exchange between the CC and the environment exerts on the possibility of an LHP start-up. It lies in the fact that at low heat loads the tendency to the approaching of the corresponding curves ΔT and ΔT_{nucl} is observed only at the initial stage of a start-up, during the process of formation of ΔT and ΔT_{nucl}. From here on their values remain unchanged. It can be seen that all the ensuing time the distance between the curves does not decrease, the curves are parallel to each other. It means that a start-up at such heat loads is impossible. A different situation arises when there is no heat exchange between the CC and the environment. This can be judged by comparing Figs. 8 and 9. As for the curves $\Delta T = f(\tau)$ in Fig. 9, their behavior is similar to that of the curves $\Delta T = f(\tau)$ in Fig. 8, whereas the curves $\Delta T_{\text{nucl}} = f(\tau)$ behave differently. It is seen that when $\alpha_{\text{amb}} = 0$, no stabilization of ΔT_{nucl} takes place. There is a constant decrease in ΔT_{nucl}. Such a change in the behavior of ΔT_{nucl} is caused by a constant decrease in the evaporator temperature, which is explained by the fact that all the heat supplied to the evaporator is accumulated in it and leads to constant warming up of the evaporator. Despite the fact that for different heat loads the rate of change of ΔT_{nucl} is different, the fact of approaching of the corresponding curves $\Delta T_{\text{nucl}} = f(\tau)$ and $\Delta T = f(\tau)$ is evident. The striving for the reduction of the distance between the curves ΔT and ΔT_{nucl} is a positive factor, which makes it possible to expect that at any heat loads Q the value of ΔT in prospect is sure to exceed the value of ΔT_{nucl}, and the condition (4) will be fulfilled. This circumstance means that in principle a start-up can be realized at any, even very low heat loads. However, it should be born in mind that this process may take a long time. Besides, such a start-up will take place at sufficiently high evaporator temperatures. It should be remembered that it is not alloys permissible because of the limitations imposed on the maximum temperature of the object being cooled, which may not exceed a certain critical value.

It is worthwhile to mention quite an interesting fact revealed in analyzing the results of a model experiment. The point is that it is possible to ensure the fulfillment of the condition (4) during a start-up not only at the cost of an increase in the temperature drop ΔT, but also at the cost of a decrease in the value of the superheat ΔT_{nucl}. Which of these two mechanisms for one or another situation will be predominant and exert the crucial effect on the start-up success depends on the heat load density, and also on the conditions of heat exchange between the CC and the environment.

Similar calculations were performed for an evaporator made of materials with a low thermal conductivity. The dependences $\Delta T_{\text{nucl}} = f(\tau)$ and $\Delta T = f(\tau)$ for different heat loads with allowance for the heat exchange between the CC and the environment are shown in Fig. 10. The results

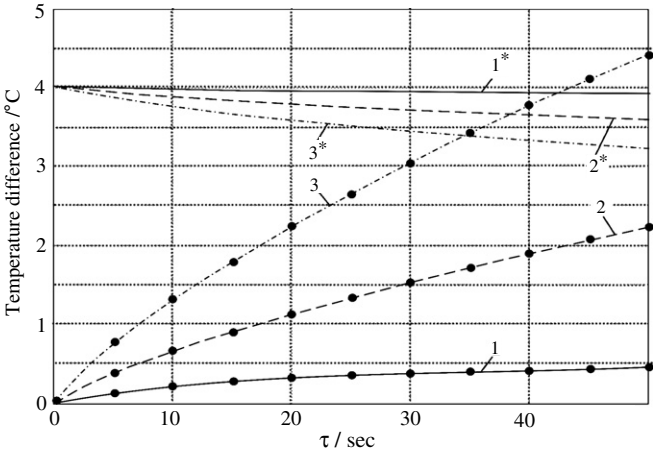

Fig. 10. Formation of temperature drop ΔT (curves 1, 2, 3) and variation of ΔT_{nucl} (curves 1^*, 2^*, 3^*) in the process of heating of SS/Ti – evaporator at different heat loads: 1, 1^* – $Q = 1$ W; 2, 2^* – $Q = 5$ W; 3, 3^* – $Q = 10$ W. The working fluid is water. The compensation chamber is not heat-insulated.

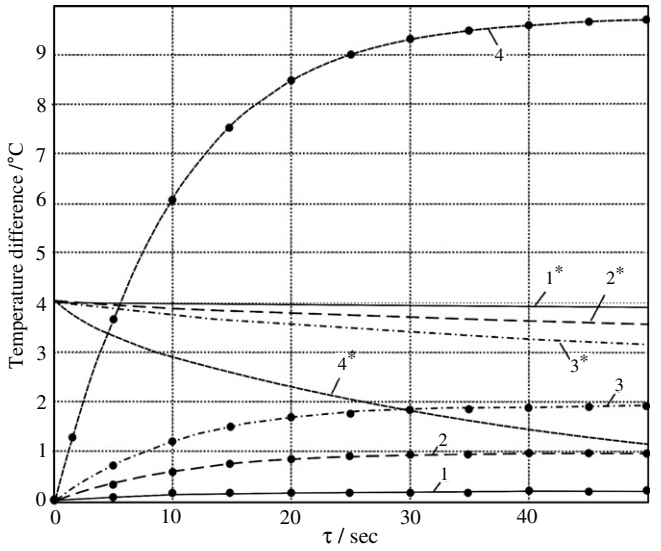

Fig. 11. Formation of temperature drop ΔT (curves 1, 2, 3, 4) and variation of ΔT_{nucl} (curves 1^*, 2^*, 3^*, 4^*) in the process of heating of SS/Ti – evaporator at different heat loads: 1, 1^* – $Q = 1$ W; 2, 2^* – $Q = 5$ W; 3, 3^* – $Q = 10$ W; 4, 4^* – $Q = 50$ W. The working fluid is water. The compensation chamber is heat-insulated.

of a numerical experiment for a thermally insulated CC are presented in Fig. 11. Water was used as a working fluid.

The graphs 10 and 11 show a decrease in the minimum heat load for evaporators with a low thermal conductivity. Besides, a considerable decrease is noted in the time of "expectation" of boiling-up. Thus, for instance, for an SS–Ti evaporator with a thermally insulated CC at a heat load of 50 W the "expectation" time is about 5 s (Fig. 11), whereas for a Cu–Cu evaporator it exceeds 70 s (Fig. 9). From this it follows that preference should be given to low thermal conductivity wicks. Comparing calculated curves for high-thermal conductivity and low-thermal

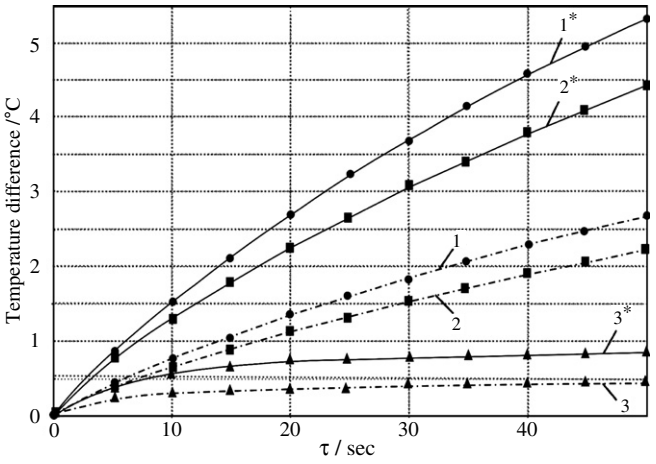

Fig. 12. Formation of temperature difference ΔT in the process of heating of SS/Ti – evaporator for different working fluids: 1, 1* – acetone; 2, 2* – water; 3, 3* – ammonia. Curves 1, 2, 3 for $Q = 5$ W; curves 1*, 2*, 3* for $Q = 10$ W.

conductivity evaporators obtained in identical conditions of heat exchange with the environment, one can note that the corresponding curves behave similarly. In this case changes are observed only in the values of ΔT and ΔT_{nucl}.

The results of a numerical experiment on the effect of thermophysical properties of various working fluids on heat-transfer processes in the evaporator were also obtained. Calculations were made as working fluids in LHPs, namely, for water, acetone and ammonia. The results presented in Fig. 12 show the changes in the temperature drop ΔT in the process of warming up of an evaporator of stainless steel with a titanium wick at heat loads equal to 5 and 10 W for three working fluids. According to the graph the highest temperature drops can be obtained with acetone as a working fluid. Ammonia has the lowest values of ΔT.

6. Conclusion

The initial stage of an LHP start-up has been simulated for the most problematic prestart situation, which is characterized by the absence of liquid in the central core and filled vapor removal channels. Based on an analysis of the results of numerical investigation of a start-up with overshoot, we can formulate the following conclusions:

1. External factors have a considerable effect on heat exchange processes in the evaporator during a start-up. Among such factors, first of all, are the conditions of heat exchange between the compensation chamber and the environment, and also the value of the heat load supplied to the evaporator.
2. Thermophysical characteristics of the working fluid and the structural materials influence the inhomogeneity of the evaporator temperature field during a start-up, the value of the minimum start-up heat load and start-up time.
3. A numerical experiment has shown that there is a range of relatively low heat loads, at which the minimum superheat required for liquid boiling-up in the vapor removal channels of the wick cannot be achieved, and therefore it becomes impossible to realize an LHP start-up. This supports the statement that there exists the lower boundary of the range of transferred heat loads made on the basis of experimental data. For this reason the minimum heat load may really be regarded as one of the main operating characteristics of an LHP.
4. The initiation of liquid boiling-up in the vapor removal channels in the process of an LHP start-up may be ensured both at the cost of formation of an inhomogeneous temperature field in the evaporator and at the cost of a decrease in the value of the superheat required for the formation of a viable vapor bubble with dimensions comparable with those of the cross-section of vapor removal channels.

Acknowledgement

This work was supported by the Russian Foundation for Basic Research, Grant No. 05-08-01180.

References

[1] Yu.F. Maidanik, Yu.G. Fershtater, Theoretical basis and classification of loop heat pipes and capillary pumped loops, in: Proceedings of the 10th International Heat Pipe Conference, Stuttgart, Germany, 1997.
[2] Yu.F. Maidanik, N.N. Solodovnik, Yu.G. Fershtater, Investigation of dynamic and stationary characteristics of a loop heat pipe, in: Proceedings of the 9th International Heat Pipe Conference, Albuquerque, USA, 1995.
[3] D. Gluck, C. Gerhart, S. Stanley, Start-up of a loop heat pipe with initially cold evaporator, compensation chamber and condenser, in: Proceedings of the 11th International Heat Pipe Conference, Tokyo, Japan, 1999, pp. 36–41.
[4] J. Rodriguez, M. Pauken, A. Na-Nakornpanom, Transient characterization of a propylene loop heat pipe during start-up and shutdown, in: Proceedings of the 30th ICES/European Symposium on Space Environmental Control Systems, 2000.
[5] J. Ku, L. Ottenstein, T. Kaya, Testing of a loop heat pipe subjected to variable accelerating forces, Part 1: start-up, in: Proceedings of the 30th ICES/European Symposium on Space Environmental Control Systems, 2000.
[6] J. Ku, Start-up of a loop heat pipe – a revisit, in: Proceedings of the International Two-Phase Thermal Control Technology Workshop, 2001.
[7] M. Nikitkin, Self-starting behavior of an LHP, in: Proceedings of the International Two Phase Control Technology Workshop, 2002.
[8] V. Kiseev, Transient and start-up behavior of loop heat pipe due to gravity, in: Proceedings of the 12th International Heat Pipe Conference, Moscow, Russia, 2002, pp. 114–119.
[9] Y. Chen, M. Groll, R. Mertz, Yu.F. Maydanik, Steady-state and transient performance of a miniature loop heat pipe, in: Proceedings of the 3rd International Conference on Microchannels and Minichannels, Toronto, Canada, 2005 (Paper No. ICMM2005-75120).
[10] R.G. Sudakov, Investigation of nonsteady and oscillatory operating mode of loop heat pipes, Ph.D. Thesis, Ural Technical University, Yekaterinburg, 2004, p. 100 (in Russian).

[11] M. Chernysheva, Yu. Maydanik, J. Ochterbeck, Numerical investigation of transient process in a cylindrical loop heat pipe evaporator during start-up, in: Proceedings of the International Two-Phase Thermal Control Technology Workshop, Noordwijk, Netherlands, September 2003.
[12] S. Zinna, M. Marengo, G.E. Cossali, Numerical simulation of a propylene LHP: stationary and start-up conditions, in: Proceedings of the 14th International Heat Pipe Conference, Florianopolis, Brazil, 2007.
[13] V.P. Skripov, Metastable Liquids, Halsted Press, New York, 1974.
[14] J.T. Zhang, B.X. Wang, Effect of capillarity at liquid–vapor interface on phase change without surfactant, Int. J. Heat Mass Transfer 45 (2002) 2689–2694.